SOCIAL ISOLATION INDUCED BEHAVIOURAL AND MICROSTRUCTURAL DIFFERENCES IN YOUNG MICE

By

Bingzhang Wu

Supervisor: Dr. Christine Tardif

Department of Biological and Biomedical Engineering

McGill University, Montreal

December 2022

A thesis submitted to McGill University in partial fulfillment of the requirements of the degree of Master of Engineering

Table of Contents

List of Figures

Abstract

Myelin is a molecular bilayer composed of proteins and lipids that insulates axons and facilitates neural functions, such as communication and metabolism. At certain time points in development, myelin forms to stabilize favourable synaptic connections, and the myelin remains plastic and adaptive throughout an organism's lifetime in response to environmental stimuli. The mechanisms behind these associations are not well understood, and animal models are used to study the relationship between experience in the brain and myelin plasticity. Through the social isolation (SI) deprivation paradigm, hypomyelination can be induced in the prefrontal cortex (PFC). Hypomyelination elicits a PFC-dependent behavioural phenotype that encompasses altered sociability and increased anxiogenic behaviour. The complexity of the dynamic nature of adaptive myelination can be captured non-invasively and quantified *in vivo* using magnetic resonance imaging (MRI). The consequences of SI during the development of young mice were investigated with the goal of reproducing behavioural alterations of previous studies, exploring sex differences in vulnerability, capturing the subtle differences in the brain *in vivo* using MRI.

A total of 43 mice, with 22 controls (10 female) and 21 SI mice (11 female), were weaned at postnatal day (PN) 21 and isolated for 6 weeks before being subjected to behaviour tests and MRI scans. SI mice showed decreased sociability (male $p = 0.00028$; female $p = 0.039$) and increased anxiogenic behaviour (male $p = 0.0024$; female $p = 0.047$), with effect size for male mice being greater than female mice. MRI did not reveal global and local differences in brain volume between groups. ROI analysis of PFC magnetization transfer saturation, an index of myelin, revealed significant differences in

multiple ROIs in the male mice but not in female mice. These results suggest there was SI-induced hypomyelination in the PFC after 6 weeks of SI and female mice were more resilient to SI when compared to the male mice. This work supports the use of MRI in longitudinal studies of SI and recovery strategies in mouse models to study the causal relationship between myelin and behaviour.

Résumé

La myéline est une bicouche moléculaire composée de protéines et de lipides qui isole les axones et facilite les fonctions neuronales, telles que la communication et le métabolisme. À certains moments du développement, la myéline se forme pour stabiliser les connexions synaptiques favorables, et la myéline reste plastique et adaptative tout au long de la vie d'un organisme en réponse aux stimulis environnementaux. Les mécanismes qui sous-tendent ces associations ne sont pas bien compris, et des modèles animaux sont utilisés pour étudier la relation entre l'expérience dans le cerveau et la plasticité de la myéline. Le paradigme de l'isolement social (IS) permet d'induire une hypomyélinisation dans le cortex préfrontal (CPFC). L'hypomyélinisation provoque un phénotype comportemental dépendant du CPF qui comprend une altération de la sociabilité et une augmentation des comportements anxiogènes. La complexité de la nature dynamique de la myélinisation adaptative peut être saisie de manière non invasive et quantifiée in vivo à l'aide de l'imagerie par résonance magnétique (IRM). Les conséquences de l'IS au cours du développement de jeunes souris ont été étudiées dans le but de reproduire les altérations comportementales des études précédentes, d'explorer les différences de vulnérabilité entre les sexes et de saisir les différences subtiles dans le cerveau in vivo en utilisant l'IRM.

Un total de 43 souris, dont 22 témoins (10 femelles) et 21 souris SI (11 femelles), ont été sevrées au jour postnatal (PN) 21 et isolées pendant 6 semaines avant d'être soumises à des tests de comportement et à des examens IRM. Les souris IS ont montré une diminution de la sociabilité (mâle $p = 0,00028$; femelle $p = 0,039$) et une augmentation du comportement anxiogène (mâle $p = 0,0024$; femelle $p = 0,047$), l'ampleur de l'effet étant plus importante chez les souris mâles que chez les souris femelles. L'IRM n'a pas révélé de différences globales et locales du volume cérébral entre les groupes. L'analyse de la saturation de transfert de magnétisation, un indice de la myéline, a révélé des différences significatives dans plusieurs régions du cortex préfrontal chez les souris mâles mais pas chez les souris femelles. Ces résultats suggèrent une hypomyélinisation induite par l'IS dans le CPF après 6 semaines d'IS et que les souris femelles étaient plus résistantes à l'IS que les souris mâles. Ce travail soutient l'utilisation de l'IRM dans les études longitudinales de l'IS et des stratégies de récupération dans les modèles de souris pour étudier la relation causale entre la myéline et le comportement.

Acknowledgments

I would like to thank my supervisor Christine Tardif for the unyielding support and encouragement that she has provided throughout every stage of my project, especially during the pandemic. I extend my gratitude to David Rudko, the members of the Tardif Lab, and the staff at the MNI's Center of Neurological Disease Models for their generous aid, support, and guidance. Thank you to Daryan Chitsaz (Kennedy Lab) for the insights into immunohistochemistry. Thank you to Gabriel Devenyi who helped with the MRI image processing, to Thomas Stroh who shared his lab space and materials. Thank you to Marius Tuznik for the great efforts and technical support during the long hours of image acquisition. Finally, thank you to my family and Rebecca for their love and companionship.

Contribution of Authors

This thesis is the original work of William (Bingzhang) Wu, supervised by Dr. Christine Tardif. Behavioural data collection and analyses were performed by the author. Magnetic resonance imaging was performed by the author and Marius Tuznik with the help of Dr. David Rudko. MRI imaging processing and analysis was performed by the author. Perfusion fixation was performed by the author, with help from Daryan Chitsaz.

List of Abbreviations

ACAd	Dorsal anterior cingulate area
ACAv	Ventral anterior cingulate area
CNS	Central nervous system
CoBrA	Computational Brain Anatomy
DBM	Deformation-based morphometry
DNA	Deoxyribonucleic acid
DWI	Diffusion weighted imaging
EPI-DA	Echo planar imaging double-angle
FLASH	Fast low angle shot
FRP	Frontal pole
ILA	Infralimbic area
MBM	MICe-build-model
MBP	Myelin basic protein
MO	Motor Area
MRI	Magnetic resonance imaging
MT	Magnetization transfer
MTR	Magnetization transfer ratio
MTsat	Magnetization transfer saturation
ODC	Oligodendrocyte
OPC	Oligodendrocyte progenitor cell
ORB	Orbital area
PBS	Phosphate buffered saline
PD	Proton density
PFA	Paraformaldehyde
PFC	Prefrontal cortex
PL	Prelimbic area
PLP	Proteolipid protein

PN	Post-natal day
RF	Radio frequency
ROI	Region of interest
SI	Social isolation
VFA	Variable flip angle
WM	White matter

1. Introduction

Myelin is a bilayer composed of lipids and proteins that originate from the oligodendrocyte cells. It coils around an axon and forms a compact sheath to act as an insulator. Myelin sheaths serve to stabilize the axon, facilitate neural communication via saltatory conduction, and support neuron function. The process of myelination is adaptive. Experiences and environmental factors can change the amount and structure in the brain throughout the lifetime of an organism (Baraban et al., 2016).

Depravation paradigms such as social isolation (SI) impact the amount of myelin in the rodent brain. Previous studies have demonstrated that SI leads to hypomyelination in the mouse brain, and a critical period has been identified in the development of the mouse brain during which myelination of the prefrontal cortex (PFC) is most vulnerable to SI with irreversible effects (Makinodan et al., 2012). This SI-induced hypomyelination is accompanied by a behavioural phenotype that consists of decreased sociability (Matthews et al., 2016; Okada et al., 2015; Pais et al., 2019) and increased anxiogenic behaviour (Lander et al., 2017; Makinodan et al., 2012). The impact of the SI paradigm is different between the male and female mice. Female mice have shown to be less vulnerable to the effects of SI, but overall research on SI female mice is lacking (Fone & Porkess, 2008; Hinton et al., 2019; Noschang et al., 2021; Pietropaolo et al., 2008), and the molecular mechanisms behind the relationship between adaptive myelination and experience are not well understood. Animal models are needed to study the relationship in greater detail, including the impact of sex. Furthering the understanding of adaptive myelination could provide insight to psychiatric disorders such as schizophrenia, anxiety, and depression

that have been associated with hypomyelination (Andersen & Teicher, 2008; Kokkosis et al., 2022; Matsumoto et al., 2019; Regenold et al., 2007).

The dynamic nature of adaptive myelination can be captured non-invasively using magnetic resonance imaging (MRI), and specifically magnetization transfer (MT) imaging (Helms et al., 2008; Steven D. Wolff & Robert S. Balaban, 1989). Being a clinical tool, MRI is the ideal tool for translational research on myelin plasticity in health and disease. Furthermore, it offers a whole brain longitudinal view of adaptive myelination, albeit at a resolution of 1.0-2.0mm in mice and 0.5-2.0mm in humans. MT imaging has been used to evaluate myelin content in mice *in vivo* in many previous studies (Fatemi et al., 2011; Jelescu et al., 2016; Turati et al., 2015), and it offers the same potential to study SI-induced myelin changes. Therefore, having an imaging protocol for high resolution MT saturation (MTsat) maps sensitive enough to capture myelin changes is a unique opportunity to study adaptive myelination in mice.

In this project, through a six-week SI paradigm, MRI is used to detect the subtle differences in PFC myelin density between the adolescent individually-housed SI mice and control socially-housed mice, which are housed in cages of three or more littermates. Both male and female mice are used to evaluate sexual dimorphism in relation to the SI paradigm. The imaging results are related back to the behavioural phenotypes through the use of sociability and anxiogenic behavioural tests. This study helps further our knowledge of the relationship between adaptive myelination, experience, and behaviour relative to sex in mice.

2. Background

2.1. Myelin Structure and composition

The myelin sheath consists mainly of bimolecular layers of lipids (70-85% by mass) and proteins (15-30% by mass) (Quarles et al., 2006). Most of the ultrastructural details currently known about myelin are based on electron microscopy imaging studies. Myelin takes the form of multilayered stacks with periodic structure of alternating electron-dense and light layers (Figure 1), which are known as the major dense line and the interperiod line respectively (Aggarwal et al., 2011). The membranes in each of these layers are compacted, resulting in a periodicity of 12 nm. In a typical myelin sheath of 15 μm in length, up to 40 layers are observed. Between two myelin sheaths is the node of Ranvier that is between 0.8- to 1.1- μm-wide (Stadelmann et al., 2019) (Figure 1). The node of Ranvier is where action potentials regenerate through the voltage-gated ion channels, and each nodal region is typically covered by astrocytic processes.

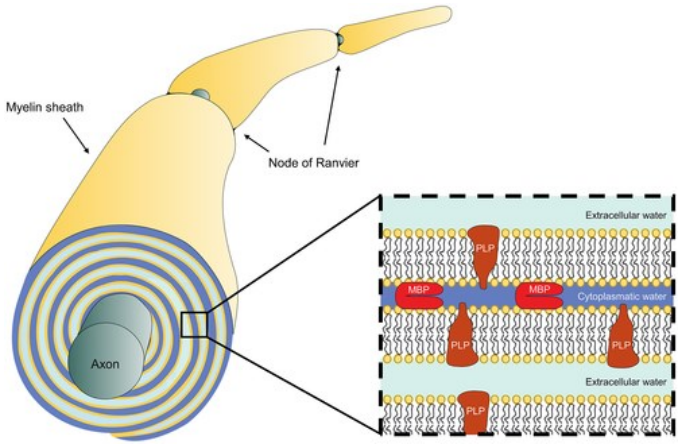

Figure 1: The organization of axonal myelination. A myelin sheath surrounding an axon is shown along with the double bilayer structure consisting of oligodendrocyte cell membranes. Myelin basic protein (MBP) creates adherence between layers and proteolipid protein (PLP) maintains extracellular shape of myelin (Piredda et al., 2021).

2.2. Functions of Myelin

Neurons are the fundamental units of the brain and the nervous system. Neurons receive, process, and propagate information throughout the brain, and communicate by transmitting electrical signals called action potentials that may be propagated over lengths up to 2 m and speeds up to 100 m/s (Hudspeth et al., 2013). Neuronal networks need to be highly coordinated, function in equilibrium, and transmit signals efficiently, and these functions are supported and facilitated by glial cells such as oligodendrocytes and the myelin they form.

The term myelin, derived from the Greek myelos after bone marrow, was coined by Virchow in 1854. Since then, several functions of myelin have been unravelled. Beyond myelin's metabolic coupling and regulation of axons, the primary function of myelin is to facilitate saltatory conduction of nerve impulses, which enables fast and efficient action potential propagation compared with unmyelinated fibers of the same dimensions (Susuki, 2010). To enable saltatory conduction, myelin tightly seals the axon, acting as an electrical insulator. This is to prevent leakage of the action potential beneath the myelin sheath, thus leading the action potential to leap from one unmyelinated node of Ranvier to the next, where high concentration of voltage-gated ion channels can regenerate the action potential (Poliak & Peles, 2003; Susuki & Rasband, 2008). Saltatory conduction in myelinated fibers is known to transmit impulses up to 100-fold faster than unmyelinated fibers, and without myelinated axons, depolarizing action potentials may attenuate below the threshold of activation or even be blocked before reaching the terminal button (Purves et al., 2001). This is observed in MBP deficient mice, such as the shiverer mice, which produce less myelin and the myelin that is produced in irregularly composed of loosely

compacted myelin lamellae (Roach et al., 1985). In these myelin-deficient mice, most axonal surfaces lack myelin entirely, and this causes them to begin exhibiting tremors shortly after birth that progressively worsens until their premature deaths (Stadelmann et al., 2019; Uschkureit et al., 2000).

On a broader scale, the quantity of myelination varies between neurons, resulting in precisely coordinated conduction timings (Fields, 2015). From providing proper responses to sensory stimuli to maintaining intrinsic oscillatory rhythms, myelin facilitates all nervous system communication (Pajevic et al., 2014).

2.3. Myelin formation during neurodevelopment

In the CNS, oligodendrocyte progenitor cells (OPCs) make up four percent of the cell population in grey matter and eight to nine percent of the cell population in white matter (Dawson et al., 2003; Tomlinson et al., 2016). OPCs migrate from the neuraxis to proliferate in the CNS during gestation. In rodents, myelin begins to form around 10-12 days postnatally, and the rate of myelination reaches the maximum at about 20 days of age (Quarles et al., 2006). From that point on, myelin continues to accumulate, but at a decreasing rate throughout adulthood, and remains adaptive. In humans, very little myelin is present at birth, but myelination occurs rapidly during the first 2 years of life as OPCs differentiate into mature oligodendrocyte cells (ODCs). The ODC processes form the myelin sheaths. Each ODC process coils around an axon until the two extracellular leaflets adhere to one another, and compaction occurs as membrane-binding proteins are integrated into the newly formed myelin sheath (Figure 2). The entire process is regulated by the signalling between glial cells and axons, and following development, this two-way transmission keeps the ODCs, neuron, and myelin healthy (Taveggia et al., 2010)).

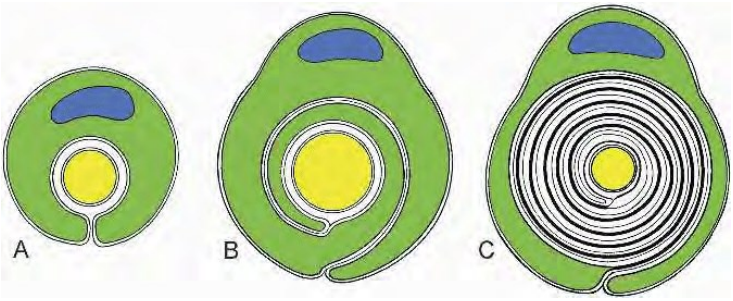

Figure 2: Stages in the development of the myelin sheath of a peripheral axon, as seen in transverse sections. (A) shows the initial formation of the leaflets, which elongates (B) and then becomes compact myelin (C) by exclusion of extracellular fluid and cytoplasm (Kiernan, 2007).

There are two phases of myelination: intrinsic and adaptive. Intrinsic myelination follows a very predictable chronological and topographic progression that is genetically predefined (Bechler et al., 2018). It begins with areas dedicated to basic homeostasis, progresses to areas in command of more complex tasks, and finally concludes with areas required for the highest cognitive processes such as the PFC (Brody et al., 1987). Myelination occurs in a proximal to distal direction within a neural pathway, and from the center to the poles within a brain region (Stadelmann et al., 2019).

2.4. Adaptive Myelin

Myelination is modulated by neuronal activity (Gibson et al., 2014) and experience (Figure 3) (Kaller et al., 2017). It occurs according to the requirements of the neuronal network and could lead to interindividual variability in myelination (Dubbioso et al., 2021; Karahan et al., 2022). Myelin remodeling occurs along single axons, influencing conduction times. Old sheaths can be replaced with new ones and unmyelinated axons can become myelinated. Myelinated axons, on the other hand, can be altered adaptively to coordinate communication with the CNS. The potential for adaptive myelination varies between brain regions, neurons, and circuits (Baraban et al., 2016). For instance, decreased magnitude of adaptive myelination occurs in most single-direction information

pathways, such as the optic nerve, that are optimised for very fast conduction times (Stadelmann et al., 2019). In contrast, neuronal networks in the cortex need to be finely tuned to synchronizing firing patterns, so axons in the cortex are subject to continuous experience-dependent adaptive myelination.

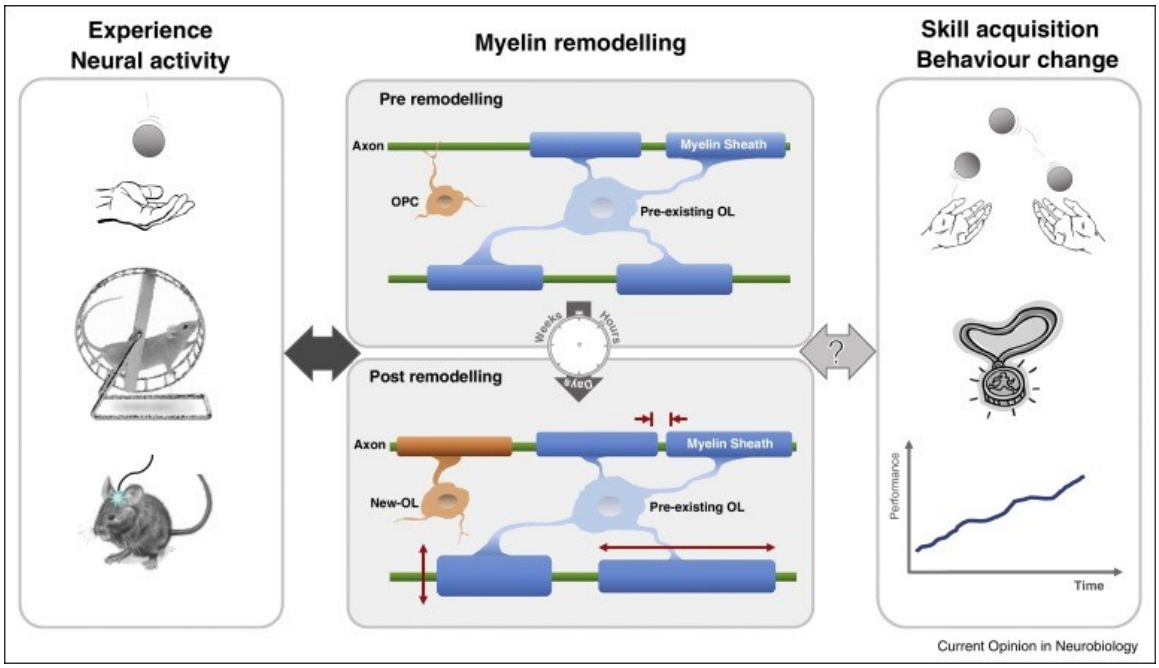

Figure 3: Myelination can be dynamically remodelled by neural activity and experience even during adulthood (Kaller et al., 2017).

Early evidence found for the existence of adaptive myelination was from the results of human neuroimaging studies. Changes in white matter were discovered upon learning new motor tasks, such as practicing piano, playing baduk, or juggling (Bengtsson et al., 2005; Lee et al., 2010; Scholz et al., 2009). Histological or electron microscopy investigations can be used to assess changes in myelination and myelin ultrastructure or adaptive myelination patterns in experimental animals. In rodents, enrichment paradigms such as voluntary exercise on running wheels and fine motor training encourage the generation of more oligodendrocytes and new myelin sheaths (McKenzie et al., 2014;

Tomlinson et al., 2016). Conversely, deprivation paradigms lead to decreased myelination (Liu et al., 2012). Collectively, these paradigms show that myelin biogenesis is influenced by experience and environmental factors.

2.5. Social Isolation-induced hypomyelination

SI is a form of social experience shutdown, such as neglect and social rejection. The SI deprivation paradigm has been shown to cause altered neurocircuitry, behavioural phenotypes, reduced myelin thickness, changes in myelin gene transcripts, specifically NG3 transcripts in the PFC, a part of the brain that controls complex emotional and cognitive activity, as well as aberrant ODC architecture with fewer branches (Liu et al., 2012; Makinodan et al., 2012). Reduced nuclear chromatin compaction and increased histone acetylation in the PFC after prolonged isolation of 8 weeks provide evidence for isolation-induced epigenetic alterations (Liu et al., 2012), and SI has been demonstrated to influence multiple neuronal circuitry and signalling pathways, such as the hypothalamic-pituitary-adrenal (HPA) stress axis (Hansen et al., 2020; Maes et al., 2011; Spiers et al., 2015).

Hypomyelination in the mouse brain caused by SI is most notable in the PFC. The prefrontal cortex has been shown to be a center for emotional regulation and modulation of social behaviors (Groenewegen & Uylings, 2000; Liu et al., 2016; Yizhar et al., 2011). It is also involved in many advanced cognitive tasks and goal-directed behaviours (Buschman & Miller, 2014; Miller, 2000). Anxiety, depressive-like behaviours, and social dysfunction are a few of the psychiatric traits that are linked to dysregulation of neuronal activity in this region (Bicks et al., 2015; Chaudhury et al., 2013; Saitoh et al., 2014; Suzuki et al., 2016; Yizhar et al., 2011). In mice, the PFC is especially susceptible

to SI-induced hypomyelination during the critical period after post-natal day (PN) 21, a period during which myelin accumulates at the fastest rate under normal developmental conditions (Makinodan et al., 2012; Quarles et al., 2006). The period between PN 21 and 35 is equivalent to young adolescence in mice. Similar to humans, this is a time of major structural reorganization and neuronal system remodeling (Agoglia et al., 2017). Synaptic connections are stabilized, refined, and pruned during this time (Palanza, 2001; Quarles et al., 2006), making this period important for the proper development of myelinated fibers.

The manifested behavioural phenotypes associated with SI are a decrease in sociability and an increase in anxiogenic behaviour, as expected from altered neuronal activity in the PFC. These changes are irreversible in juvenile mice isolated during the critical period from PN 21 to 35 (Makinodan et al., 2017; Makinodan et al., 2012). Conversely, mice that are isolated after this period can regain regular biological and behavioural phenotypes through social reintegration. Adult mice that undergo prolonged SI (8 weeks) also demonstrate these biological and behavioural phenotypes, but these changes are reversible (Liu et al., 2012). Together, the evidence comes to show that the deprivation of social stimuli would alter the normal course of brain development.

These disruptions in neural circuity make SI rodents a powerful model for human psychiatric phenotypes, including depressive-like behavior (Amiri et al., 2015; Koike et al., 2009), social deficits (Koike et al., 2009; Okada et al., 2015) and anxiety behaviors (Amiri et al., 2015; Lander et al., 2017). Studying SI-induced hypomyelination has the potential to link the changes in myelination to these human psychiatric disorders.

2.6. Studying myelin in vivo

Both *ex vivo* and *in vivo* methods are used to study myelination. *Ex vivo* myelin quantification techniques such as protein histology are myelin-specific, but these techniques are generally highly invasive or terminal, non-clinical, and limited in the potential for longitudinal studies within subjects. The response of individual cell types observed in *ex vivo* studies may not be extrapolated to tissues, and the lack of longitudinal data makes it difficult to study the impact of experience on adaptive myelination over the entire lifespan of an organism. To study this level of complexity and the dynamic nature of myelination requires *in vivo* methods.

A range of imaging methods for rodent models have been used to study myelin *in vivo*. Optical imaging techniques such as fluorescence imaging can be used in rodent models to collect quantitative data. Coherent anti-Stokes Raman scattering microscopy uses intrinsic molecular vibrations to resolve myelinated axons in the mouse brain (Fu et al., 2008). For such imaging techniques, a cranial window must be surgically implemented to image subcortical structures in the rodent model (Aswendt et al., 2014). Non-imaging techniques, mainly chemical lesion models, such as using cuprizone and lysolecithin, can be used to study toxin-induced focal demyelination in the CNS. The major disadvantage of these techniques is their invasive and preclinical nature, which limits their translational impact.

MRI is a clinical tool that can capture high resolution whole-brain images non-invasively, which sets it apart from other *in vivo* techniques. It can be used to acquire data at various stages of development within a single subject, allowing longitudinal studies to be

conducted. Furthermore, being a clinical tool, the use of MRI in the study of myelin maximizes the translational impact.

2.7. Magnetic Resonance Imaging of Rodents

MRI can create high resolution images of the brain through the use of a strong static magnetic field, spatial magnetic field gradients, and radio frequency (RF) pulses. Based on detecting the changes in the rotational axis of protons in the water that makes up biological tissues, MRI uses powerful magnets to create a strong magnetic field that compels protons in the body to align with that magnetic field. The protons are excited and spin out of equilibrium, struggling against the magnetic field's pull, when a RF pulse is emitted through the subject inside the MRI machine. RF coils can detect the energy produced as the protons realign with the magnetic field when the RF field is switched off.

MR imaging is most often used to measure signal from hydrogen protons, which are typically found in bulk water or fat. Tuned RF pulses are used to generate a signal from these protons, which is then spatially encoded into images using magnetic field gradients. By varying the timings of the application of RF pulses and gradients, one can sensitize the MR signal to generate contrast between tissues due to differences in the microstructural and chemical environment of the measured water, similar to how stains can be used to generate contrast in sectioned tissue samples due to different properties of tissue microstructure (Alexander et al., 2011; McRobbie et al., 2006)..

Early imaging studies that found evidence for the existence of rodent adaptive myelination mainly used diffusion-weighted imaging (DWI) (Dong et al., 2004; Harsan et al., 2006; Mori et al., 2001; Nair et al., 2005). DWI has been utilized to measure tissue parameters in many human neuroimaging studies of white matter microstructure. It is a

method used to map and characterize the three-dimensional diffusion of water molecules in nerve fibers, capable of characterizing microstructural architecture (Alexander et al., 2007; Basser et al., 1994). However, DWI is sensitive but not specific to myelination, its measurements can be influenced by axon density, caliber, cell swelling, fiber architecture, and other microstructural factors (Beaulieu, 2014; Heath et al., 2018). Although DWI remains a useful and sensitive tool for assessing brain microstructure, the method is not myelin specific.

The magnetization transfer (MT) effect is an MR-based method for estimating myelin content in CNS tissues. Protons bound to big macromolecules are not immediately visible in MR images due to their extremely short T2 transverse relaxation time. The signal from these sources decays before it can be captured by imaging sequences. This pool of macromolecular protons has a far wider range of resonance frequencies, which can be used to selectively saturate them. MT is the physical process by which these macromolecules and their closely associated water molecules cross-relax with protons in the free water pool (Grossman, 1994; Steven D Wolff & Robert S Balaban, 1989). By assuming most macromolecule content in the CNS is myelin, MT can be used as an indirect measurement of the myelin content of the tissue (Henkelman et al., 2001).

In MT imaging, an RF pulse is administered on resonance with a wide bandwidth, or at an offset to the water resonance frequency. The energy given to macromolecules exchanges with free water to restore equilibrium, leading to an attenuation in the water signal measured. In MT ratio (MTR) imaging, an image with an off-resonance MT saturation pulse applied is normalized by an image taken without the MT saturation pulse, while holding other parameters constant (Fralix et al., 1991). There is good

agreement between MTR and histology of rat demyelination and remyelination brain experiments (Deloire-Grassin et al., 2000), and validation studies have shown correlation between MTR and myelin content (Dousset et al., 1995; Dousset et al., 1992), but this semi – quantitative metric is inherently impacted by the tissue's T1 relaxation time and the RF transmit B1 field ($B1^{+}$) inhomogeneity (Rowley et al., 2021).

Compared to MTR, MT saturation (MTsat) requires an additional image collected with no MT-weighting and increased T1-weighted contrast generated using a higher flip angle. It was developed as an improvement to MTR (Hagiwara et al., 2018) by decoupling MTR from T1, thus it offers a measure that minimizes the T1 dependence and is less sensitive to $B1^{+}$ inhomogeneities. The images used to construct MTsat maps have been shown to exhibit low intra-scanner variability, especially for white matter (WM), thus the scan-rescan variability between different scans does not pose a major challenge (Cooper et al., 2020; Gracien et al., 2020)

MTsat provides an alternative to fully quantitative techniques, and with increased WM to gray matter (GM) contrast relative to that in MTR maps (Helms et al., 2008; Lema et al., 2017). MTsat has also been shown to correlate more with disability metrics than MTR in patients with multiple sclerosis and has shown high correlations with the fraction of protons bound to macromolecules (Campbell et al., 2018; Lema et al., 2017), thus it has the potential to further insights into adaptive myelination.

3. Objectives:

The objective of this research project is to use a non-invasive imaging tool to investigate the relationship between social isolation-induced adaptive myelination and behaviour in mice, while accounting for sex differences. The specific aims are:

1. To replicate the social isolation-induced behavioural phenotype in wild type mice;
2. To use a quantitative MRI protocol to map cross-sectional differences in myelination between socially housed and socially isolated mice *in vivo* and relate the differences to the behavioural phenotype;
3. To investigate sex differences in the relationship between adaptive myelination and behaviour in this paradigm.

Hypotheses:

1. I hypothesize that socially isolated mice will show decreased sociability, increased anxiogenic behaviour, and decreased myelin content in the PFC measured using MRI.

2. I hypothesize that male mice will be more vulnerable to the deprivation paradigm than female mice and exhibit increased behavioural phenotype and decreased myelin.

4. Methodology

4.1. Mice

All experimental mice were bred from C57BL/6J wildtype mice purchased from Jackson Laboratories. In-house breeding was performed to avoid potential confounds that might result from the transportation of young mice. The C57BL/6J strain was selected for this study because it was previously used to study SI-induced myelin plasticity by other laboratories (Liu et al., 2012) and to demonstrate the existence of critical periods crucial to myelin development in young-adolescent mice (Makinodan et al., 2012). All mice were housed at The Montreal Neurological Institute's Centre of Neurological Disease Models in humidity-and-temperature-controlled rooms with *ad libitum* access to food and water and a 12-hour light-dark cycle. The behavioural data and MRI scans included 22 controls (10 female), and 21 SI mice (11 female).

4.2. Social Isolation Paradigm

Mice were weaned, ear-tagged, and kept as social controls (3-4 mice per cage) or in isolation (1 mouse per cage) for six weeks starting on postnatal day (PN) 21. At PN 21 and PN 63, mice were weighed. During the five days leading up to PN 63, every mouse was handled by the same investigator for 5 minutes per day so that unexpected handling did not affect the outcomes of the behavior results. Behavioural assays and MRI scans, described in detail below, were performed starting on PN 63. Each assay was performed 24 hours apart from the previous test. 10 mice (4 males, of which 1 is isolated, and 6 females, of which 3 are isolated) were sacrificed, and perfusion fixed after the scan. Their brains were kept for subsequent histological analysis that is not within the scope of this thesis.

4.3. Behavioural Tests

Crawley's Sociability Test (Moy et al., 2004) and the Elevated-Zero Maze (Shepherd et al., 1994) were used to assess sociability and anxiogenic behaviour respectively. The path taken by the mice and time spent in each region of interest during the behaviour tests were recorded and scored using the HVS Image video tracking and analysis system (2018.8.895 version). Prior to every experiment, the animals were transported to the behaviour room and habituated for 30 minutes. Mice were transported from their cages onto the behaviour apparatus via enclosed carboard cylinders to minimize anxiety prior to testing. The behaviour apparatus was cleaned with 70% ethanol solution and Quatricide after each use for sterilization and elimination of olfactory confounds.

4.4. Crawley's Sociability Test

Sociability was evaluated using a three-chamber box (60 x 40cm) with transparent walls and an opening on each of the two dividing walls as illustrated in figure 4. Mice could freely move among the three chambers once the openings were unblocked. Two identical cylindrical cages were placed at the center of each side chamber, with one cage being designated to hold the intruder mice. The cages allow for air exchange but limited physical contact between the experimental mouse and the intruder mouse. The intruder mouse was the same strain, age, and sex as the experimental mouse, and they had similar weight. During each trial, the experimental mouse was initially transported into the central empty chamber and was allowed to habituate for five minutes. The intruder mouse was then placed into the designated cylindrical cage, which alternated sides after each trial, and the openings to the side chambers were unblocked. The experimental mouse was allowed to freely explore the three chambers for ten minutes. The total path length,

average speed, time spent with intruder and within each chamber, urination, and number of fecal boluses were recorded.

4.5. Elevated-Zero Maze

Anxiogenic behaviour was evaluated using the Elevated-Zero Maze. The behaviour apparatus consists of an elevated circular platform that is divided into quadrants. Two opposing quadrants have high walls while the other two opposing quadrants are entirely exposed, as shown in Figure 4. The Elevated-Zero Maze is similar to the Elevated-Plus Maze (Braun et al., 2011) but eliminates the ambiguity of the central region between the exposed and walled arms. During each trial, the experimental mouse was placed into a walled quadrant, alternating sides between each trial, and the mouse was allowed to freely explore the maze for five minutes. The total path length, average speed, time spent within the covered quadrants, number of quadrant entries, number of quadrants explored, urination, and number of fecal boluses were recorded.

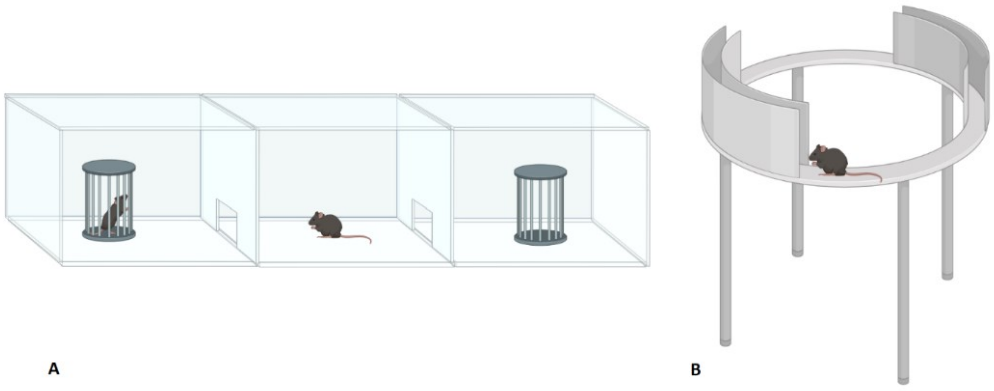

Figure 4: A) Crawley's Sociability Test B) Elevated 0-Maze

4.6. Magnetic Resonance Imaging

The mice were scanned in vivo on the small bore 7 Tesla Bruker Pharmascan (Bruker 70/16) with a clear bore size of 16cm and operating on Paravision 5.1 at the Genome Quebec Innovations Centre. Each mouse was sedated in a sedation chamber at 4% isoflurane and 300 ml/min flowrate. The sedated mouse was transferred into the scanner room and positioned into a nose cone. A respiration sensor was placed underneath the animal, and the animal was secured to a slidable bed. The temperature and respiration of the animal was continuously monitored. The isoflurane vaporizer was set between 0.5-2.5% at 400 ml/min, and the warm air was set between 30-31°C. The animal was injected with 1 ml of warm saline before and after each scanning session.

Three different 3D FLASH MR images were acquired at 200 um isotropic resolution. The T1-, PD-, and MT-weighted scans were achieved by the selection of the repetition time (TR) and the appropriate flip angle (FA). TR/FA = 15 ms/25° for the T1w scan and 28 ms/5° for the PDw and the MTw scans. MT-weighting was achieved by applying an off-resonance Gaussian-shaped RF pulse (8 ms duration, 9.8μT, 2 kHz frequency offset from water resonance). The above scans were used to calculate the MTsat maps to estimate brain tissue myelin content.

4.7. Perfusions

Mice were perfused with 4% PFA in 0.1M PBS at a rate of 10ml/min. Brains were then dissected and submerged in PFA overnight at 4°C, soaked in 30% sucrose solution overnight, flash-frozen in Tissue Tek O.C.T. at -40°C, and stored at -80°C for potential future use.

4.8. Image processing

The cross-sectional mouse MRI data was pre-processed using MICe-build-model (MBM) developed by the Computational Brain Anatomy (CoBrA) Laboratory. MTw images were used as input for MBM. The MBM registration pipeline is a multi-stage process that aligns individual mouse brain images to a common space (Chakravarty et al., 2016), the DSURQE atlas (Dorr et al., 2008; Richards et al., 2011; Steadman et al., 2014; Ullmann et al., 2013). The whole-brain deformation-based morphometry (DBM) analysis uses the Jacobian determinant of the non-linear transformations to the common space to detect local differences in volume between SI and control groups, and within males and females in each condition. MTsat images were also resampled into the common space for whole brain voxel-based analysis.

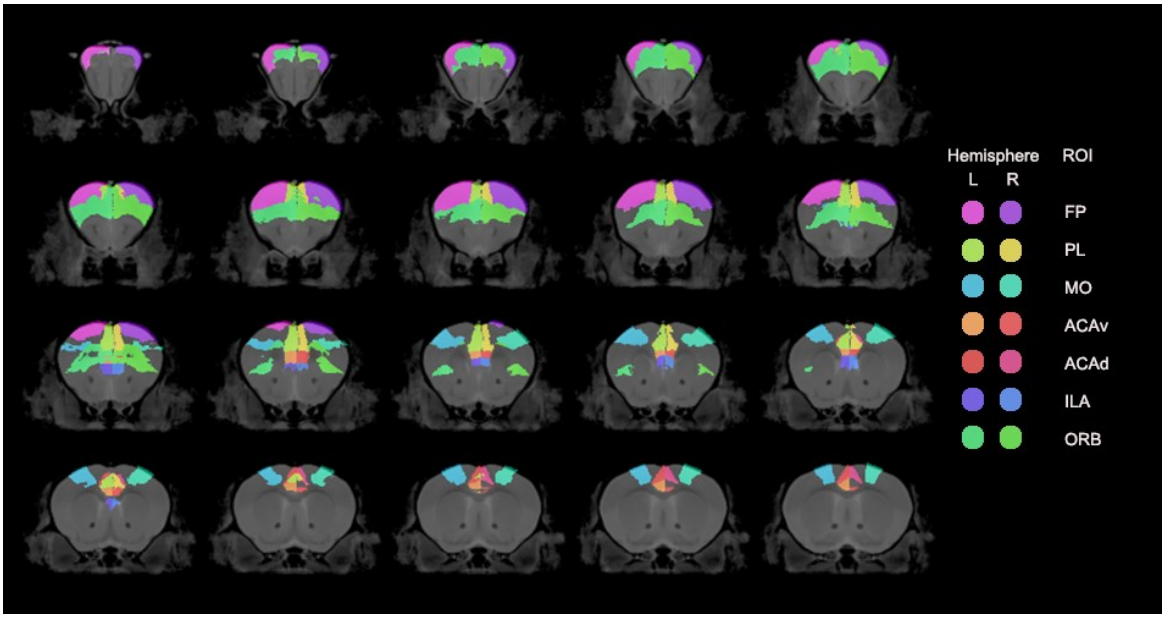

Figure 5: PFC regions of interest created from the DSURQE reference atlas (Dorr et al., 2008; Richards et al., 2011; Steadman et al., 2014; Ullmann et al., 2013)

The following regions of interest (ROI) were defined in the PFC using the unisex DSURQE atlas, as shown in Figure 5: the prelimbic area (PL), infralimbic area (ILA), dorsal and ventral anterior cingulate areas (ACAd, and ACAv respectively), frontal pole

(FRP), and orbital areas (ORB) (Le Merre et al., 2021).The motor area (MO) was selected as a control region due to previous findings that this region shows little social experience-dependent changes (Makinodan et al., 2012). The volume and average MTsat was evaluated for each ROI. Voxel-based and ROI-based statistics were carried out using R (version 3.6.3) and RMINC (version 1.5.2.1).

4.9. Statistical analysis

Shapiro-Wilk test for normality and Levene's test for homogeneity of variances were used to check assumptions. Student's t-tests and non-parametric Mann-Whitney U test for independent samples were used to identify group (SI or control) and sex differences in sociability and anxiogenic behaviour. Linear models were used to further investigate the fixed effects of group (SI or control) and sex on sociability and anxiogenic behaviour.

Partial least squares (PLS), an associative, multivariate method for relating two data sets to each other by finding the optimal weighted linear combinations of variables that maximally covary with each other (Hansen et al., 2020; Krishnan et al., 2011; McIntosh & Lobaugh, 2004; Zeighami et al., 2019), was used to further investigate the relationship between the behaviour dataset, which consists of parent pair, sex, weight PN 21, weight PN 63, sociability and zero maze average speed, sociability and zero maze zone entries, sociability time with intruder, number of urination and defecation, zero maze total path length, zero maze zones used, and zero maze time spent covered, and the MTsat-ROI dataset. Permutation testing and bootstrap resampling were set to 5000 repetitions and applied to assess latent variable (LV) significance and reliability. The number of the LV corresponds to the rank of the covariance matrix (Guma et al., 2021; Zeighami et al., 2019). PLS analysis (Hansen et al., 2020) was carried out using Python (version 3.6).

5. Results

5.1. Decrease in Sociability Observed in SI Mice

Sociability was measured as the percentage of time spent in the chamber that housed the social intruder mouse compared to the total time of 10 minutes of the trial. The datasets are normally distributed and have homogeneity of variance. Student's t-test showed that SI mice spent significantly less time in the chamber with the social intruder compared to the control mice for both male ($t = 4.44$, $p = 0.00028$) and female ($t = 2.24$, $p = 0.039$) mice (Figure 6). The effect size for the male mice ($d = 1.80$) is larger than the female mice ($d = 0.85$), but no significant sex difference in the effects of SI on sociability was observed ($t = 0.63$, $p = 0.54$). Linear models revealed no major effects of litter, parent pair, weight, and locomotor activity on sociability ($p's > 0.05$).

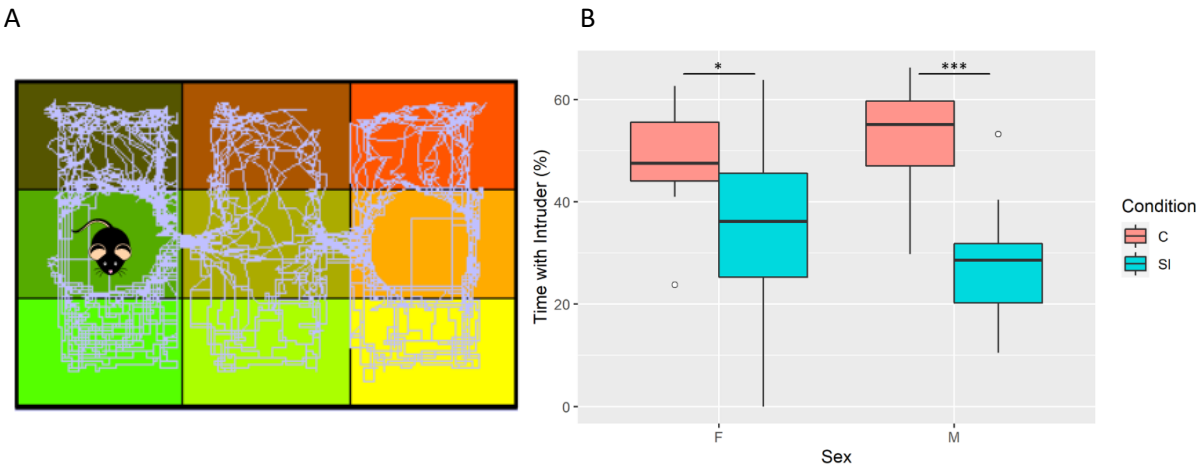

Figure 6: Sociability test results

A) Example of HVS Image tracking output.

B) Significant difference was observed in the sociability behaviour between conditions in both males and females (x̄C Female = 47.8 ± 10.9%; x̄SI Female = 32.7 ± 19.3%; x̄C Male = 51.7 ± 12.2%; x̄SI Male = 28.2 ± 12.5%).

5.2. Increased Anxiogenic Behaviour Observed in SI Mice

The level of anxiogenic behaviour was measured as the percentage of time spent in the covered quadrants of the elevated-zero maze compared to the total time of 5 minutes of the trial. The datasets are normally distributed and have homogeneity of variance. Student's t-test revealed that SI mice spent significantly more time in the covered quadrant compared to the control mice for both male ($t = -3.48$, $p = 0.0024$) and female ($t = -2.15$, $p = 0.047$). The effect size for the male mice ($d = -1.38$) is larger than that for the female mice ($d = -0.86$), but no significant sex difference in the effects of SI on anxiogenic behaviour was observed ($t = -1.50$, $p = 0.15$) (Figure 7). Linear models revealed no effects of litter, parent pair, weight, and locomotor activity on anxiogenic behaviour (p's > 0.05).

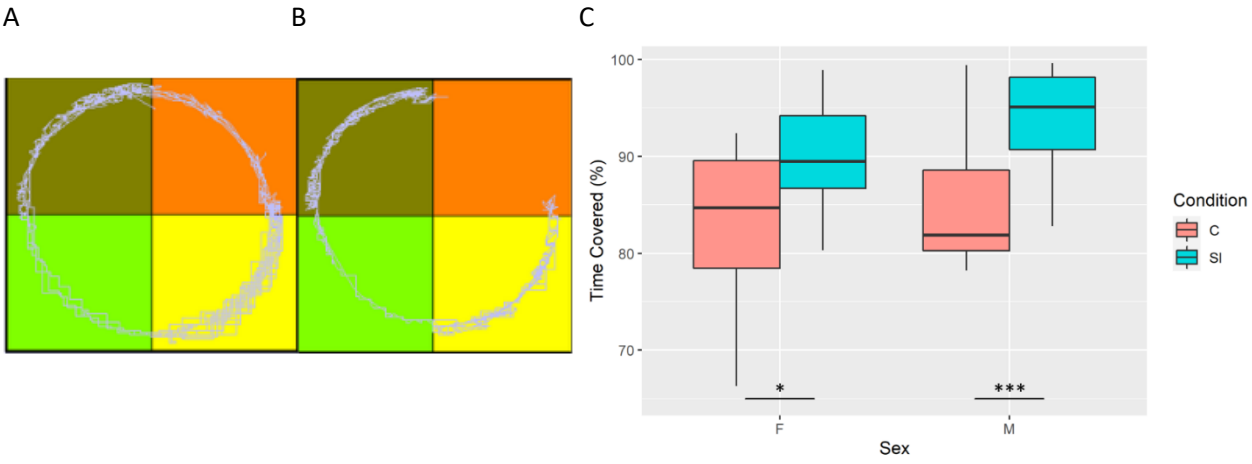

Figure 7: Elevated-Zero Maze test results

A) Example of HVS Image tracking output for the control condition.

B) Example of HVS Image tracking output for the isolated condition

C) Significant difference was observed in the anxiogenic behaviour between conditions in both males and females (x̄C Female = 82.58 ± 8.9%; x̄SI Female = 89.8 ± 6.1%; x̄C Male = 84.8 ± 6.3%; x̄SI Male = 93.7 ± 5.7%).

5.3. Decreased MTsat in regions of the prefrontal cortex

The exploratory voxel-based whole brain analyses did not show any significant results between socially isolated and control mice. DBM analysis did not reveal any significant local structural differences between the two conditions analyzed as a group and analyzed by individual sex. Whole-brain voxel-based analysis of MTsat intensity showed no differences between conditions. Group average MTsat can be seen in Figure 8.

ROI analysis of MTsat intensity revealed lower MTsat for the SI condition compared to controls for the ROIs of $ACAv_L$ ($p = 0.045$, false discovery rate (FDR) < 10%), $ACAv_R$ ($p = 0.049$, FDR < 10%), FRP_L ($p = 0.036$, FDR < 10%), FRP_R ($p = 0.0017$, FDR < 5%), ILA_R ($p = 0.0019$, FDR < 5%), ORB_L ($p = 0.041$, FDR < 10%), and ORB_R ($p = 0.038$, FDR < 10%) (Figure 9). The MO, serving as a control ROI, saw no difference between conditions. Interestingly, when the male and female data was analyzed separately, the differences were not significant for the female mice, but remained significant for the male mice. Analysis of ROI volumes did not show significant differences.

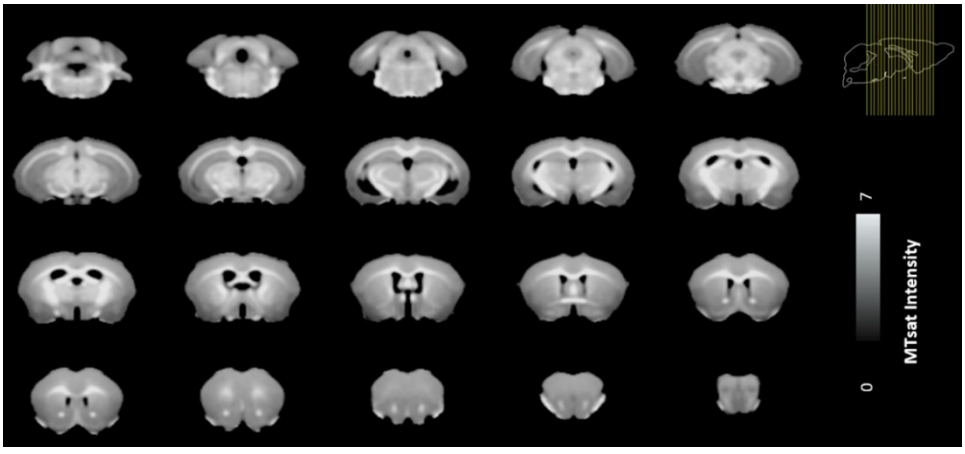

Figure 8: Coronal view of group average MTsat images showing nice contrast between white and grey matter.

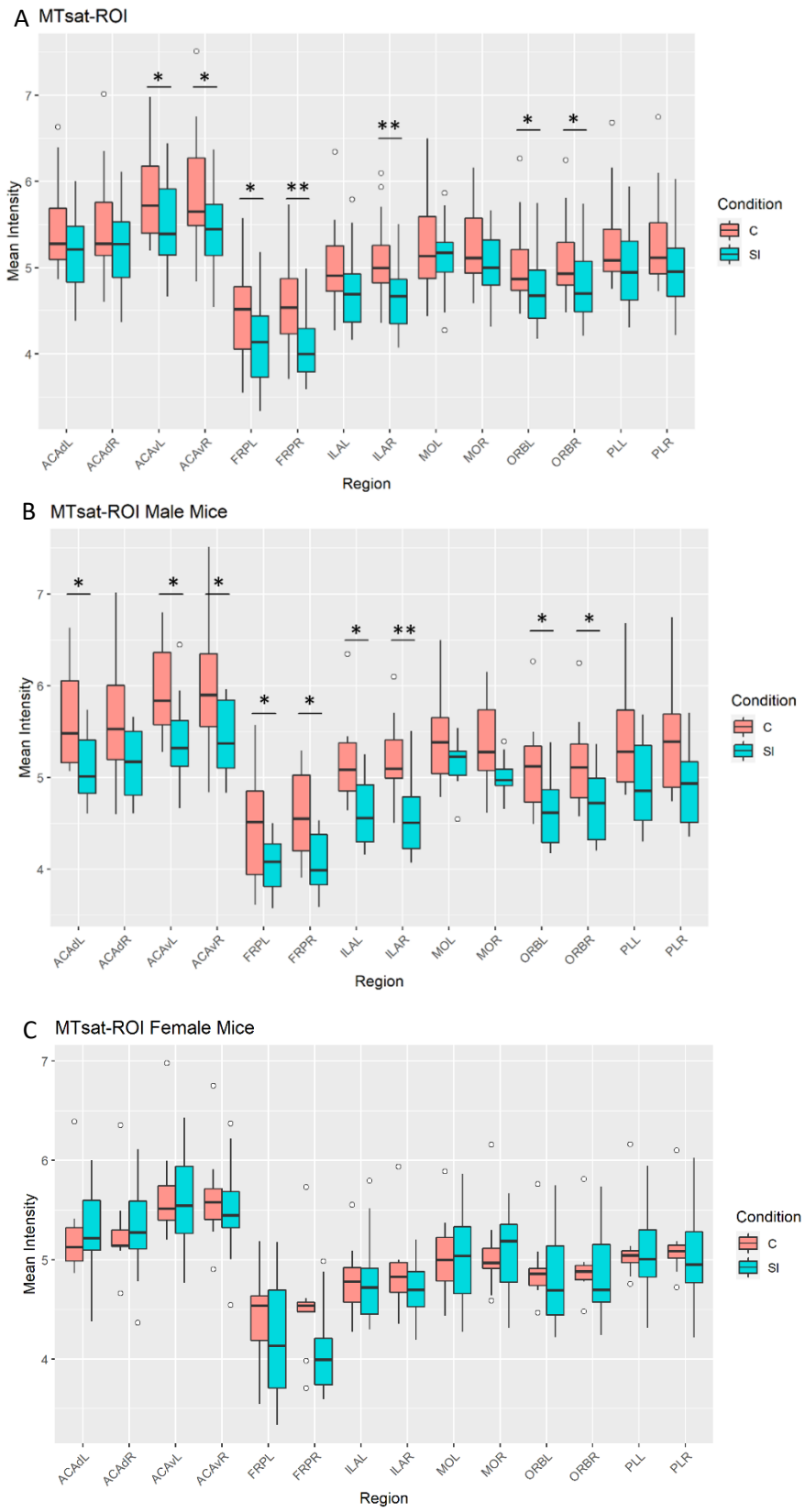

Figure 9: MTsat ROI-based analysis results

A) Examining condition without accounting for sex. Lower mean MTsat intensity observed in SI mice for ACAvL, ACAvR, FRPL, FRPR, ILAR, ORBL, ORBR.

B) Male mice had lower mean MTsat intensity for ACAdL, ACAvL, ACAvR, FRPL, FRPR, ILAL, ILAR, ORBL, ORBR.

C) No significant difference between conditions in female mice.

Regions of Interest: the dorsal and ventral anterior cingulate areas (ACAd, and ACAv respectively), frontal pole (FRP), infralimbic area (ILA), motor area (MO), orbital areas (ORB), and prelimbic area (PL).

** $p < 0.05$;*

*** $p < 0.01$;*

**** $p < 0.00$.*

5.4. Partial least squares

The PLS analysis revealed one statistically significant LV relating the MTsat-ROI intensities and the behavioural dataset ($p = 0.001$). LV-1 is the optimal linear combination of variables that accounts for 95% of the shared covariance between the behavioural and MTsat measures (Figure 10 A). More specifically, for the five measures with unidirectional confidence intervals (CI), weight at PN 63 was the main contributor to LV-1 ($R = 0.60$, 95% CI [0.30,0.78]) followed by sociability time with intruder ($R = 0.36$, 95% CI [0.08, 0.58]), zero-maze number of urination ($R = - 0.24$, CI [-0.43, -0.02]), zero-maze zone used ($R = 0.32$, 95% CI [0.08, 0.56]), and zero-maze time covered ($R= - 2.59$, 95% CI [-0.53, -0.03]) (Figure 10 B). Brain score and behaviour score correlation can be seen in Figure 10 C. Correlation between brain and behaviour suggests that a decrease in MTsat is associated with a pattern of behavioural impairment. After evaluating the behaviour measures correlated with MTsat, Student's t-test showed no difference in weight at PN 63 between conditions, whether examined as individual sexes or both male and female mice together, and significant difference between sexes ($t = - 2.78$, $p = 0.0089$). Analysis of the number of quadrants used for the zero-maze showed that SI mice used significantly fewer quadrants than control mice ($t = 5.1$, $p= 0.000086$), and there was no significant difference in the number quadrants used between male and female mice.

A

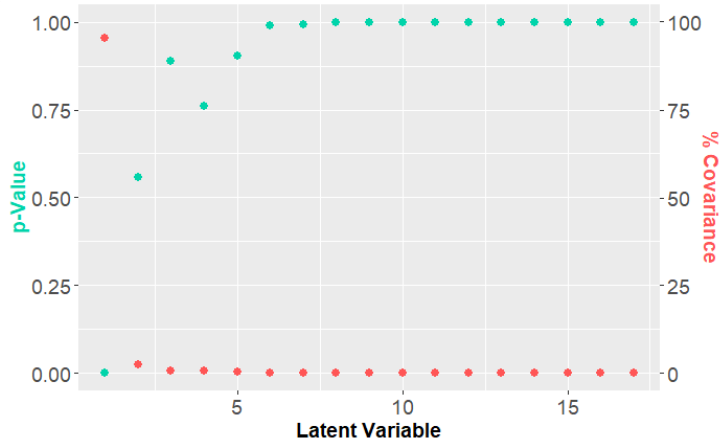

B

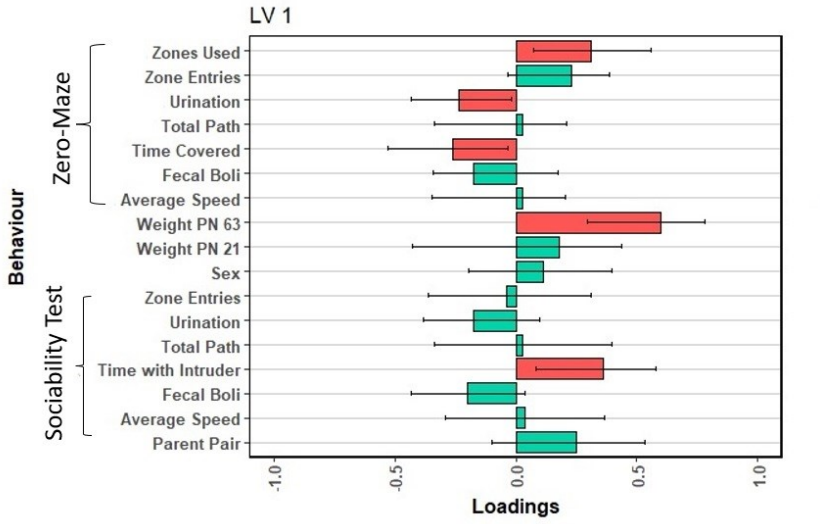

C

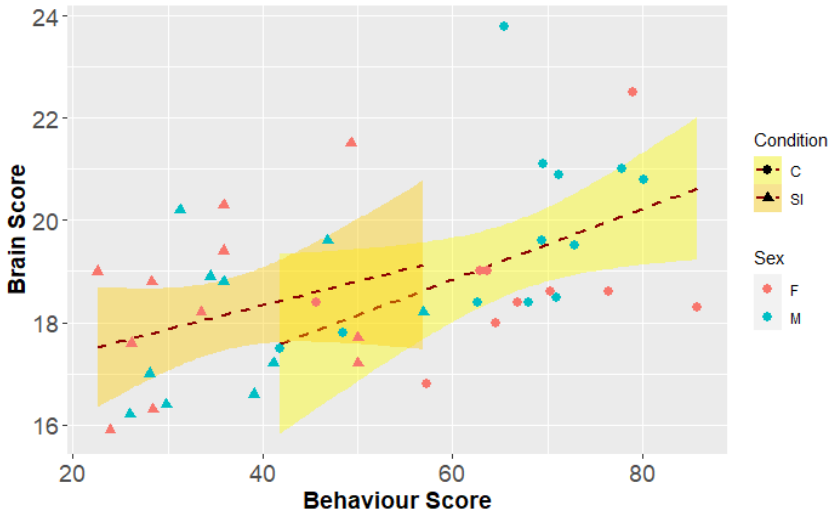

Figure 10: PLS results

A) P-value of each latent variable and their respective percentage of covariance.

B) LV 1 obtained from PLS analysis. The effect sizes are estimated using singular value decomposition analysis and the confidence intervals are calculated by bootstrapping. Red bars indicate unidirectionality of 95% CI. (Z = Zero-Maze; S = Sociability)

C) Individual mouse brain versus behaviour score, color coded by sex, shape coded by condition, and with a trend line per condition.

6. Discussion

The goal of this study was to utilize a non-invasive imaging technique to detect minute adaptive changes in myelin content of the mouse brain in response to a social isolation paradigm. We replicate Liu et al.'s and Makinodan et al.'s findings that SI induces hypomyelination in the PFC of mice, as well as behavioural deficits including reduced sociability and increased anxiogenic behaviour (Liu et al., 2012; Makinodan et al., 2012). This study demonstrates that the SI-induced hypomyelination of the PFC can be captured with myelin-sensitive MT imaging, with imaging findings correlating to behaviour data. Stronger effects for both behaviour and imaging results are observed in male mice, but similar trends are shown in female mice.

6.1. Significant differences in sociability and increase in anxiogenic behaviour

In this study, sociability was significantly decreased and anxiogenic behaviour significantly increased in isolated mice as compared to the control mice, and a greater effect size was observed for the male mice compared to the female mice. The findings are consistent with previous research that also reported decreased sociability (Liu et al., 2012; Makinodan et al., 2017; Makinodan et al., 2012; Okada et al., 2015) and increased anxiety (Amiri et al., 2015; Fone & Porkess, 2008; Lander et al., 2017) as a result of the SI paradigm. However, it is crucial to note that the majority of studies to date used only male mice, leaving it unclear to what extent sex affects susceptibility to SI. According to the results of this study, female mice appear to be somewhat resilient to the effects of SI on sociability and anxiogenic behavior. Previous research indicates that oestrogen in females may act as a neuroprotective mechanism, strengthening females' resistance to stress, particularly social stress (Ferdman et al., 2007; Palanza et al., 2001). Similar to our

findings, in the few studies that have observed SI in females, differences between sexes were recorded in both biology and behaviour in response to SI (Chadda & Devaud, 2004; Hinton et al., 2019; Lukkes et al., 2009; Pietropaolo et al., 2008; Rodgers & Cole, 1993; Weiss et al., 2004). Furthermore, sex differences are observed in several human psychiatric disorders (Qiu et al., 2018), where symptoms are often more severe in men than in women (Pietropaolo et al., 2008).

6.2. Lower myelin content in the prefrontal cortex of isolated mice detected using MRI

There was no difference detected in whole-brain analysis of brain morphology between conditions. For whole brain voxel-wise analysis of MTsat, also no significance between the two condition was detected. Methods to correct for multiple comparisons in whole brain voxel-based analysis, such as false discovery rate, are well known for the inflation of Type II error (Lieberman & Cunningham, 2009) and limit the ability to correctly detect differences in smaller regions. Since a priori hypothesis is present, there is the need and justification to consider the analysis of the specific ROIs that make up the PFC for the ability to maximize the identification of subtle differences (Poldrack, 2007).

Analysis of PFC ROIs shows significantly decreased MTsat intensity in most ROIs but not in the MO area that served as a control. This corresponds with our hypothesis. But interestingly, the majority of the difference between conditions was contributed solely by the male mice. If the female mice are evaluated alone, there would be no significant difference between conditions. The decreased sociability and increased anxiogenic behaviour in the female mice suggest change in the brains of the isolated mice, but this change could be much more subtle compared to the isolated male mice, as indicated by

the lower effect size of the female mice's behavioural results when compared to the male mice's results. In a previous pilot study, which utilized a shorter 2-week SI paradigm, a similar observation was reported: a significant difference in the elevated-zero maze was observed between the conditions for the male mice, but no change in any measured brain metric was reported. The small change in myelination required for the manifestation of a significant impact on behaviour could be too subtle to be detected by the imaging protocol.

6.3. PLS analysis confirms contribution of behavioural results

PLS analysis confirms that sociability test results, and anxiogenic test results significantly contribute to the covariance between the behavioural and brain datasets. It also reveals that weight at PN 63 is the biggest contributor of the overall covariance in MTsat.

The average weight of the male mice at PN 63 is significantly greater than that of the female mice. Brain size affects the amount the ability of MRI to capture subtle differences in myelination. The image resolution limits the ability to capture differences in smaller structures, and brain size impacts the signal-to-noise ratio of the images acquired due to the coil fill factor. Since the female mice have much lower weight and brain size, the amount of myelin is lower than the males and the signal-to-noise ratio is lower as well. This could contribute to the lack of significant results in the female ROI-based analysis of MTsat.

Previous studies that reported significant myelin differences due to SI in confocal imaging results conducted longer SI paradigms and imaged much older mice (Liu et al., 2012; Liu et al., 2016; Medendorp et al., 2018), which would ensure a more pronounced effect of SI and bigger brain size for effective imaging. For future studies, longer SI

paradigms and imaging larger adult mice could help evaluate the sensitivity of the imaging protocol.

6.4. Limitations

This study demonstrated that a 6-week long isolation paradigm from PN 21 to PN 63 induces behavioural deficits in mice and induces hypomyelination in the PFC that is capturable *in vivo* with MTsat in male mice. For the female mice, behavioural deficits were weaker and trends that resemble the male mice are observed but are not statistically significant. Imaging mice at PN 65 could be insufficient time for mice to fully develop the SI phenotype. A previous study that looked at neuroanatomy development of C57BL/6J mice showed significant developmental differences between male and female mice brains, and individualization and development of the brain emerged earlier in males (Qiu et al., 2018). The differences observed between sexes may be in part due to the faster developmental trajectory of male mice. Longitudinal studies are needed to characterize the myelination trajectories of male and female mice during development.

There are additional confounds that may have impacted the results. For female mice, the estrous cycle was not controlled for, potentially introducing sex-related confounds if estrogen induces resilience to stress.

7. Conclusion

This work shows that myelin-sensitive MT imaging may detect the SI-induced hypomyelination of the PFC, with imaging results corresponding to behavioural data. Male mice exhibit stronger effects for both behavior and imaging outcomes, although female mice exhibit similar trends. The use of MRI enables the observation of such subtle

myelin changes and allows in the future for potential longitudinal paradigms of conditional knockout models to investigate the causal effect of hypomyelination on behaviour, and individual differences in susceptibility to SI and potential for recovery.

References:

Aggarwal, S., Yurlova, L., & Simons, M. (2011). Central nervous system myelin: structure, synthesis and assembly. *Trends in cell biology*, *21*(10), 585-593.

Agoglia, A. E., Holstein, S. E., Small, A. T., Spanos, M., Burrus, B. M., & Hodge, C. W. (2017). Comparison of the adolescent and adult mouse prefrontal cortex proteome. *PLoS One*, *12*(6), e0178391.

Alexander, A. L., Hurley, S. A., Samsonov, A. A., Adluru, N., Hosseinbor, A. P., Mossahebi, P., Tromp, D. P., Zakszewski, E., & Field, A. S. (2011). Characterization of cerebral white matter properties using quantitative magnetic resonance imaging stains. *Brain connectivity*, *1*(6), 423-446.

Alexander, A. L., Lee, J. E., Lazar, M., & Field, A. S. (2007). Diffusion tensor imaging of the brain. *Neurotherapeutics*, *4*(3), 316-329.

Amiri, S., Haj-Mirzaian, A., Rahimi-Balaei, M., Razmi, A., Kordjazy, N., Shirzadian, A., Mehr, S. E., Sianati, H., & Dehpour, A. R. (2015). Co-occurrence of anxiety and depressive-like behaviors following adolescent social isolation in male mice; possible role of nitrergic system. *Physiology & behavior*, *145*, 38-44.

Andersen, S. L., & Teicher, M. H. (2008). Stress, sensitive periods and maturational events in adolescent depression. *Trends in neurosciences*, *31*(4), 183-191.

Aswendt, M., Adamczak, J., & Tennstaedt, A. (2014). A review of novel optical imaging strategies of the stroke pathology and stem cell therapy in stroke. *Frontiers in cellular neuroscience*, *8*, 226.

Baraban, M., Mensch, S., & Lyons, D. A. (2016). Adaptive myelination from fish to man. *Brain Res*, *1641*(Pt A), 149-161. https://doi.org/10.1016/j.brainres.2015.10.026

Basser, P. J., Mattiello, J., & LeBihan, D. (1994). MR diffusion tensor spectroscopy and imaging. *Biophysical journal*, *66*(1), 259-267.

Beaulieu, C. (2014). The biological basis of diffusion anisotropy. In *diffusion MRI* (pp. 155-183). Elsevier.

Bechler, M. E., Swire, M., & ffrench‐Constant, C. (2018). Intrinsic and adaptive myelination—A sequential mechanism for smart wiring in the brain. *Developmental neurobiology*, *78*(2), 68-79.

Bengtsson, S. L., Nagy, Z., Skare, S., Forsman, L., Forssberg, H., & Ullén, F. (2005). Extensive piano practicing has regionally specific effects on white matter development. *Nature neuroscience*, *8*(9), 1148-1150.

Bicks, L. K., Koike, H., Akbarian, S., & Morishita, H. (2015). Prefrontal cortex and social cognition in mouse and man. *Frontiers in psychology*, *6*, 1805.

Braun, A. A., Skelton, M. R., Vorhees, C. V., & Williams, M. T. (2011). Comparison of the elevated plus and elevated zero mazes in treated and untreated male Sprague–Dawley rats: effects of anxiolytic and anxiogenic agents. *Pharmacology Biochemistry and Behavior*, *97*(3), 406-415.

Brody, B. A., Kinney, H. C., Kloman, A. S., & Gilles, F. H. (1987). Sequence of central nervous system myelination in human infancy. I. An autopsy study of myelination. *Journal of Neuropathology & Experimental Neurology*, *46*(3), 283-301.

Buschman, T. J., & Miller, E. K. (2014). Goal-direction and top-down control. *Philosophical Transactions of the Royal Society B: Biological Sciences*, *369*(1655), 20130471.

Campbell, J. S., Leppert, I. R., Narayanan, S., Boudreau, M., Duval, T., Cohen-Adad, J., Pike, G. B., & Stikov, N. (2018). Promise and pitfalls of g-ratio estimation with MRI. *Neuroimage*, *182*, 80-96.

Chadda, R., & Devaud, L. L. (2004). Sex differences in effects of mild chronic stress on seizure risk and GABAA receptors in rats. *Pharmacology Biochemistry and Behavior*, *78*(3), 495-504.

Chakravarty, M. M., Hamani, C., Martinez-Canabal, A., Ellegood, J., Laliberté, C., Nobrega, J. N., Sankar, T., Lozano, A. M., Frankland, P. W., & Lerch, J. P. (2016). Deep brain stimulation of the ventromedial prefrontal cortex causes reorganization of neuronal processes and vasculature. *Neuroimage*, *125*, 422-427.

Chaudhury, D., Walsh, J. J., Friedman, A. K., Juarez, B., Ku, S. M., Koo, J. W., Ferguson, D., Tsai, H.-C., Pomeranz, L., & Christoffel, D. J. (2013). Rapid regulation of depression-related behaviours by control of midbrain dopamine neurons. *Nature*, *493*(7433), 532-536.

Cooper, G., Hirsch, S., Scheel, M., Brandt, A. U., Paul, F., Finke, C., Boehm-Sturm, P., & Hetzer, S. (2020). Quantitative Multi-Parameter Mapping Optimized for the Clinical Routine. *Frontiers in neuroscience*, *14*. https://doi.org/10.3389/fnins.2020.611194

Dawson, M. R., Polito, A., Levine, J. M., & Reynolds, R. (2003). NG2-expressing glial progenitor cells: an abundant and widespread population of cycling cells in the adult rat CNS. *Molecular and Cellular Neuroscience*, *24*(2), 476-488.

Deloire-Grassin, M., Brochet, B., Quesson, B., Delalande, C., Dousset, V., Canioni, P., & Petry, K. (2000). In vivo evaluation of remyelination in rat brain by magnetization transfer imaging. *Journal of the neurological sciences*, *178*(1), 10-16.

Dong, Q., Welsh, R. C., Chenevert, T. L., Carlos, R. C., Maly-Sundgren, P., Gomez-Hassan, D. M., & Mukherji, S. K. (2004). Clinical applications of diffusion tensor imaging. *Journal of Magnetic Resonance Imaging: An Official Journal of the International Society for Magnetic Resonance in Medicine*, *19*(1), 6-18.

Dorr, A., Lerch, J. P., Spring, S., Kabani, N., & Henkelman, R. M. (2008). High resolution three-dimensional brain atlas using an average magnetic resonance image of 40 adult C57Bl/6J mice. *Neuroimage*, *42*(1), 60-69.

Dousset, V., Brochet, B., Vital, A., Gross, C., Benazzouz, A., Boullerne, A., Bidabe, A.-M., Gin, A.-M., & Caille, J.-M. (1995). Lysolecithin-induced demyelination in primates: preliminary in vivo study with MR and magnetization transfer. *American journal of neuroradiology*, *16*(2), 225-231.

Dousset, V., Grossman, R. I., Ramer, K. N., Schnall, M. D., Young, L. H., Gonzalez-Scarano, F., Lavi, E., & Cohen, J. A. (1992). Experimental allergic encephalomyelitis and multiple sclerosis: lesion characterization with magnetization transfer imaging. *Radiology*, *182*(2), 483-491.

Dubbioso, R., Madsen, K. H., Thielscher, A., & Siebner, H. R. (2021). The myelin content of the human precentral hand knob reflects interindividual differences in manual motor control at the physiological and behavioral level. *Journal of Neuroscience*, *41*(14), 3163-3179.

Fatemi, A., Wilson, M. A., Phillips, A. W., McMahon, M. T., Zhang, J., Smith, S. A., Arauz, E. J., Falahati, S., Gummadavelli, A., Bodagala, H., Mori, S., & Johnston, M. V. (2011). In vivo magnetization transfer MRI shows dysmyelination in an ischemic mouse model of periventricular leukomalacia. *J Cereb Blood Flow Metab*, *31*(10), 2009-2018. https://doi.org/10.1038/jcbfm.2011.68

Ferdman, N., Murmu, R., Bock, J., Braun, K., & Leshem, M. (2007). Weaning age, social isolation, and gender, interact to determine adult explorative and social behavior, and dendritic and spine morphology in prefrontal cortex of rats. *Behavioural brain research*, *180*(2), 174-182.

Fields, R. D. (2015). A new mechanism of nervous system plasticity: activity-dependent myelination. *Nature Reviews Neuroscience*, *16*(12), 756-767.
Fone, K. C., & Porkess, M. V. (2008). Behavioural and neurochemical effects of post-weaning social isolation in rodents—relevance to developmental neuropsychiatric disorders. *Neuroscience & Biobehavioral Reviews*, *32*(6), 1087-1102.
Fralix, T. A., Ceckler, T. L., Wolff, S. D., Simon, S. A., & Balaban, R. S. (1991). Lipid bilayer and water proton magnetization transfer: effect of cholesterol. *Magnetic resonance in medicine*, *18*(1), 214-223.
Fu, Y., Huff, T. B., Wang, H.-W., Wang, H., & Cheng, J.-X. (2008). Ex vivo and in vivo imaging of myelin fibers in mouse brain by coherent anti-Stokes Raman scattering microscopy. *Optics express*, *16*(24), 19396-19409.
Gibson, E. M., Purger, D., Mount, C. W., Goldstein, A. K., Lin, G. L., Wood, L. S., Inema, I., Miller, S. E., Bieri, G., & Zuchero, J. B. (2014). Neuronal activity promotes oligodendrogenesis and adaptive myelination in the mammalian brain. *Science*, *344*(6183), 1252304.
Gracien, R.-M., Maiworm, M., Brüche, N., Shrestha, M., Nöth, U., Hattingen, E., Wagner, M., & Deichmann, R. (2020). How stable is quantitative MRI? – Assessment of intra- and inter-scanner-model reproducibility using identical acquisition sequences and data analysis programs. *Neuroimage*, *207*. https://doi.org/10.1016/j.neuroimage.2019.116364
Groenewegen, H. J., & Uylings, H. B. (2000). The prefrontal cortex and the integration of sensory, limbic and autonomic information. *Progress in brain research*, *126*, 3-28.
Grossman, R. I. (1994). Magnetization transfer in multiple sclerosis. *Annals of Neurology: Official Journal of the American Neurological Association and the Child Neurology Society*, *36*(S1), S97-S99.
Guma, E., Snook, E., Spring, S., Lerch, J. P., Nieman, B. J., Devenyi, G. A., & Chakravarty, M. M. (2021). Subtle alterations in neonatal neurodevelopment following early or late exposure to prenatal maternal immune activation in mice. *NeuroImage: Clinical*, *32*, 102868.
Hagiwara, A., Hori, M., Kamagata, K., Warntjes, M., Matsuyoshi, D., Nakazawa, M., Ueda, R., Andica, C., Koshino, S., & Maekawa, T. (2018). Myelin measurement: comparison between simultaneous tissue relaxometry, magnetization transfer saturation index, and T1w/T2w ratio methods. *Scientific reports*, *8*(1), 1-12.
Hansen, J. Y., Markello, R. D., Vogel, J. W., Seidlitz, J., Bzdok, D., & Misic, B. (2020). Molecular signatures of cognition and affect. *bioRxiv*.
Harsan, L. A., Poulet, P., Guignard, B., Steibel, J., Parizel, N., Loureiro de Sousa, P., Boehm, N., Grucker, D., & Ghandour, M. S. (2006). Brain dysmyelination and recovery assessment by noninvasive in vivo diffusion tensor magnetic resonance imaging. *Journal of neuroscience research*, *83*(3), 392-402.
Heath, F., Hurley, S. A., Johansen-Berg, H., & Sampaio-Baptista, C. (2018). Advances in noninvasive myelin imaging. *Developmental neurobiology*, *78*(2), 136-151.
Helms, G., Dathe, H., Kallenberg, K., & Dechent, P. (2008). High-resolution maps of magnetization transfer with inherent correction for RF inhomogeneity and T1 relaxation obtained from 3D FLASH MRI. *Magnetic Resonance in Medicine: An Official Journal of the International Society for Magnetic Resonance in Medicine*, *60*(6), 1396-1407.
Henkelman, R., Stanisz, G., & Graham, S. (2001). Magnetization transfer in MRI: a review. *NMR in Biomedicine: An International Journal Devoted to the Development and Application of Magnetic Resonance In Vivo*, *14*(2), 57-64.
Hinton, E. A., Li, D. C., Allen, A. G., & Gourley, S. L. (2019). Social Isolation in Adolescence Disrupts Cortical Development and Goal-Dependent Decision-Making in Adulthood,

Despite Social Reintegration. *eNeuro*, *6*(5). https://doi.org/10.1523/ENEURO.0318-19.2019

Hudspeth, A. J., Jessell, T. M., Kandel, E. R., Schwartz, J. H., & Siegelbaum, S. A. (2013). *Principles of neural science*. McGraw-Hill, Health Professions Division.

Jelescu, I. O., Zurek, M., Winters, K. V., Veraart, J., Rajaratnam, A., Kim, N. S., Babb, J. S., Shepherd, T. M., Novikov, D. S., Kim, S. G., & Fieremans, E. (2016). In vivo quantification of demyelination and recovery using compartment-specific diffusion MRI metrics validated by electron microscopy. *Neuroimage*, *132*, 104-114. https://doi.org/10.1016/j.neuroimage.2016.02.004

Kaller, M. S., Lazari, A., Blanco-Duque, C., Sampaio-Baptista, C., & Johansen-Berg, H. (2017). Myelin plasticity and behaviour—connecting the dots. *Current opinion in neurobiology*, *47*, 86-92.

Karahan, E., Tait, L., Si, R., Özkan, A., Szul, M. J., Graham, K. S., Lawrence, A. D., & Zhang, J. (2022). The interindividual variability of multimodal brain connectivity maintains spatial heterogeneity and relates to tissue microstructure. *Communications biology*, *5*(1), 1-13.

Kiernan, J. A. (2007). Histochemistry of staining methods for normal and degenerating myelin in the central and peripheral nervous systems. *Journal of Histotechnology*, *30*(2), 87-106.

Koike, H., Ibi, D., Mizoguchi, H., Nagai, T., Nitta, A., Takuma, K., Nabeshima, T., Yoneda, Y., & Yamada, K. (2009). Behavioral abnormality and pharmacologic response in social isolation-reared mice. *Behavioural brain research*, *202*(1), 114-121.

Kokkosis, A. G., Madeira, M. M., Mullahy, M. R., & Tsirka, S. E. (2022). Chronic stress disrupts the homeostasis and progeny progression of oligodendroglial lineage cells, associating immune oligodendrocytes with prefrontal cortex hypomyelination. *Mol Psychiatry*, *27*(6), 2833-2848. https://doi.org/10.1038/s41380-022-01512-y

Krishnan, A., Williams, L. J., McIntosh, A. R., & Abdi, H. (2011). Partial Least Squares (PLS) methods for neuroimaging: a tutorial and review. *Neuroimage*, *56*(2), 455-475.

Lander, S. S., Linder-Shacham, D., & Gaisler-Salomon, I. (2017). Differential effects of social isolation in adolescent and adult mice on behavior and cortical gene expression. *Behavioural brain research*, *316*, 245-254.

Le Merre, P., Ährlund-Richter, S., & Carlén, M. (2021). The mouse prefrontal cortex: Unity in diversity. *Neuron*, *109*(12), 1925-1944.

Lee, B., Park, J.-Y., Jung, W. H., Kim, H. S., Oh, J. S., Choi, C.-H., Jang, J. H., Kang, D.-H., & Kwon, J. S. (2010). White matter neuroplastic changes in long-term trained players of the game of "Baduk"(GO): a voxel-based diffusion-tensor imaging study. *Neuroimage*, *52*(1), 9-19.

Lema, A., Bishop, C., Malik, O., Mattoscio, M., Ali, R., Nicholas, R., Muraro, P. A., Matthews, P. M., Waldman, A. D., & Newbould, R. D. (2017). A comparison of magnetization transfer methods to assess brain and cervical cord microstructure in multiple sclerosis. *Journal of neuroimaging*, *27*(2), 221-226.

Lieberman, M. D., & Cunningham, W. A. (2009). Type I and Type II error concerns in fMRI research: re-balancing the scale. *Social cognitive and affective neuroscience*, *4*(4), 423-428.

Liu, J., Dietz, K., DeLoyht, J. M., Pedre, X., Kelkar, D., Kaur, J., Vialou, V., Lobo, M. K., Dietz, D. M., & Nestler, E. J. (2012). Impaired adult myelination in the prefrontal cortex of socially isolated mice. *Nature neuroscience*, *15*(12), 1621-1623.

Liu, J., Dupree, J. L., Gacias, M., Frawley, R., Sikder, T., Naik, P., & Casaccia, P. (2016). Clemastine enhances myelination in the prefrontal cortex and rescues behavioral changes in socially isolated mice. *Journal of Neuroscience*, *36*(3), 957-962.

Lukkes, J. L., Watt, M. J., Lowry, C. A., & Forster, G. L. (2009). Consequences of post-weaning social isolation on anxiety behavior and related neural circuits in rodents. *Frontiers in behavioral neuroscience*, 18.

Maes, M., Galecki, P., Chang, Y. S., & Berk, M. (2011). A review on the oxidative and nitrosative stress (O&NS) pathways in major depression and their possible contribution to the (neuro) degenerative processes in that illness. *Progress in Neuro-Psychopharmacology and Biological Psychiatry*, *35*(3), 676-692.

Makinodan, M., Ikawa, D., Yamamuro, K., Yamashita, Y., Toritsuka, M., Kimoto, S., Yamauchi, T., Okumura, K., Komori, T., Fukami, S. I., Yoshino, H., Kanba, S., Wanaka, A., & Kishimoto, T. (2017). Effects of the mode of re-socialization after juvenile social isolation on medial prefrontal cortex myelination and function. *Sci Rep*, *7*(1), 5481. https://doi.org/10.1038/s41598-017-05632-2

Makinodan, M., Rosen, K. M., Ito, S., & Corfas, G. (2012). A critical period for social experience-dependent oligodendrocyte maturation and myelination. *Science*, *337*(6100), 1357-1360. https://doi.org/10.1126/science.1220845

Matsumoto, K., Fujiwara, H., Araki, R., & Yabe, T. (2019). Post-weaning social isolation of mice: a putative animal model of developmental disorders. *Journal of Pharmacological Sciences*, *141*(3), 111-118.

Matthews, G. A., Nieh, E. H., Vander Weele, C. M., Halbert, S. A., Pradhan, R. V., Yosafat, A. S., Glober, G. F., Izadmehr, E. M., Thomas, R. E., Lacy, G. D., Wildes, C. P., Ungless, M. A., & Tye, K. M. (2016). Dorsal Raphe Dopamine Neurons Represent the Experience of Social Isolation. *Cell*, *164*(4), 617-631. https://doi.org/10.1016/j.cell.2015.12.040

McIntosh, A. R., & Lobaugh, N. J. (2004). Partial least squares analysis of neuroimaging data: applications and advances. *Neuroimage*, *23*, S250-S263.

McKenzie, I. A., Ohayon, D., Li, H., Paes de Faria, J., Emery, B., Tohyama, K., & Richardson, W. D. (2014). Motor skill learning requires active central myelination. *Science*, *346*(6207), 318-322.

McRobbie, D. W., Moore, E. A., Graves, M. J., & Prince, M. R. (2006). MRI from protons to pictures. In: Cambridge University Press Cambridge.

Medendorp, W. E., Petersen, E. D., Pal, A., Wagner, L.-M., Myers, A. R., Hochgeschwender, U., & Jenrow, K. A. (2018). Altered behavior in mice socially isolated during adolescence corresponds with immature dendritic spine morphology and impaired plasticity in the prefrontal cortex. *Frontiers in behavioral neuroscience*, *12*, 87.

Miller, E. K. (2000). The prefontral cortex and cognitive control. *Nature Reviews Neuroscience*, *1*(1), 59-65.

Mori, S., Itoh, R., Zhang, J., Kaufmann, W. E., Van Zijl, P. C., Solaiyappan, M., & Yarowsky, P. (2001). Diffusion tensor imaging of the developing mouse brain. *Magnetic Resonance in Medicine: An Official Journal of the International Society for Magnetic Resonance in Medicine*, *46*(1), 18-23.

Moy, S., Nadler, J., Perez, A., Barbaro, R., Johns, J., Magnuson, T., Piven, J., & Crawley, J. (2004). Sociability and preference for social novelty in five inbred strains: an approach to assess autistic-like behavior in mice. *Genes, Brain and Behavior*, *3*(5), 287-302.

Nair, G., Tanahashi, Y., Low, H. P., Billings-Gagliardi, S., Schwartz, W. J., & Duong, T. Q. (2005). Myelination and long diffusion times alter diffusion-tensor-imaging contrast in myelin-deficient shiverer mice. *Neuroimage*, *28*(1), 165-174.

Noschang, C., Lampert, C., Krolow, R., & de Almeida, R. M. M. (2021). Social isolation at adolescence: a systematic review on behaviour related to cocaine, amphetamine and

nicotine use in rats and mice. *Psychopharmacology (Berl)*, *238*(4), 927-947. https://doi.org/10.1007/s00213-021-05777-z

Okada, R., Fujiwara, H., Mizuki, D., Araki, R., Yabe, T., & Matsumoto, K. (2015). Involvement of dopaminergic and cholinergic systems in social isolation-induced deficits in social affiliation and conditional fear memory in mice. *Neuroscience*, *299*, 134-145.

Pais, A. B., Pais, A. C., Elmisurati, G., Park, S. H., Miles, M. F., & Wolstenholme, J. T. (2019). A Novel Neighbor Housing Environment Enhances Social Interaction and Rescues Cognitive Deficits from Social Isolation in Adolescence. *Brain Sci*, *9*(12). https://doi.org/10.3390/brainsci9120336

Pajevic, S., Basser, P. J., & Fields, R. D. (2014). Role of myelin plasticity in oscillations and synchrony of neuronal activity. *Neuroscience*, *276*, 135-147.

Palanza, P. (2001). Animal models of anxiety and depression: how are females different? *Neuroscience & Biobehavioral Reviews*, *25*(3), 219-233.

Palanza, P., Gioiosa, L., & Parmigiani, S. (2001). Social stress in mice: gender differences and effects of estrous cycle and social dominance. *Physiology & behavior*, *73*(3), 411-420.

Pietropaolo, S., Singer, P., Feldon, J., & Yee, B. K. (2008). The postweaning social isolation in C57BL/6 mice: preferential vulnerability in the male sex. *Psychopharmacology (Berl)*, *197*(4), 613-628. https://doi.org/10.1007/s00213-008-1081-3

Piredda, G. F., Hilbert, T., Thiran, J. P., & Kober, T. (2021). Probing myelin content of the human brain with MRI: A review. *Magnetic resonance in medicine*, *85*(2), 627-652.

Poldrack, R. A. (2007). Region of interest analysis for fMRI. *Social cognitive and affective neuroscience*, *2*(1), 67-70.

Poliak, S., & Peles, E. (2003). The local differentiation of myelinated axons at nodes of Ranvier. *Nature Reviews Neuroscience*, *4*(12), 968-980.

Purves, D., Augustine, G., Fitzpatrick, D., Katz, L., LaMantia, A., McNamara, J., & Williams, S. (2001). Increased conduction velocity as a result of myelination. *Neuroscience*.

Qiu, L. R., Fernandes, D. J., Szulc-Lerch, K. U., Dazai, J., Nieman, B. J., Turnbull, D. H., Foster, J. A., Palmert, M. R., & Lerch, J. P. (2018). Mouse MRI shows brain areas relatively larger in males emerge before those larger in females. *Nature communications*, *9*(1), 1-15.

Quarles, R. H., Macklin, W. B., & Morell, P. (2006). Myelin formation, structure and biochemistry. *Basic neurochemistry: molecular, cellular and medical aspects*, *7*, 51-71.

Regenold, W. T., Phatak, P., Marano, C. M., Gearhart, L., Viens, C. H., & Hisley, K. C. (2007). Myelin staining of deep white matter in the dorsolateral prefrontal cortex in schizophrenia, bipolar disorder, and unipolar major depression. *Psychiatry research*, *151*(3), 179-188.

Richards, K., Watson, C., Buckley, R. F., Kurniawan, N. D., Yang, Z., Keller, M. D., Beare, R., Bartlett, P. F., Egan, G. F., & Galloway, G. J. (2011). Segmentation of the mouse hippocampal formation in magnetic resonance images. *Neuroimage*, *58*(3), 732-740.

Roach, A., Takahashi, N., Pravtcheva, D., Ruddle, F., & Hood, L. (1985). Chromosomal mapping of mouse myelin basic protein gene and structure and transcription of the partially deleted gene in shiverer mutant mice. *Cell*, *42*(1), 149-155.

Rodgers, R., & Cole, J. (1993). Influence of social isolation, gender, strain, and prior novelty on plus-maze behaviour in mice. *Physiology & behavior*, *54*(4), 729-736.

Rowley, C. D., Campbell, J. S., Wu, Z., Leppert, I. R., Rudko, D. A., Pike, G. B., & Tardif, C. L. (2021). A model‐based framework for correcting inhomogeneity effects in magnetization transfer saturation and inhomogeneous magnetization transfer saturation maps. *Magnetic resonance in medicine*, *86*(4), 2192-2207.

Saitoh, A., Ohashi, M., Suzuki, S., Tsukagoshi, M., Sugiyama, A., Yamada, M., Oka, J. I., Inagaki, M., & Yamada, M. (2014). Activation of the prelimbic medial prefrontal cortex induces anxiety-like behaviors via N-methyl-D-aspartate receptor-mediated glutamatergic neurotransmission in mice. *Journal of neuroscience research*, *92*(8), 1044-1053.

Scholz, J., Klein, M. C., Behrens, T. E., & Johansen-Berg, H. (2009). Training induces changes in white-matter architecture. *Nature neuroscience*, *12*(11), 1370-1371.

Shepherd, J. K., Grewal, S. S., Fletcher, A., Bill, D. J., & Dourish, C. T. (1994). Behavioural and pharmacological characterisation of the elevated "zero-maze" as an animal model of anxiety. *Psychopharmacology*, *116*(1), 56-64.

Spiers, J. G., Chen, H.-J. C., Sernia, C., & Lavidis, N. A. (2015). Activation of the hypothalamic-pituitary-adrenal stress axis induces cellular oxidative stress. *Frontiers in neuroscience*, *8*, 456.

Stadelmann, C., Timmler, S., Barrantes-Freer, A., & Simons, M. (2019). Myelin in the central nervous system: structure, function, and pathology. *Physiological reviews*, *99*(3), 1381-1431.

Steadman, P. E., Ellegood, J., Szulc, K. U., Turnbull, D. H., Joyner, A. L., Henkelman, R. M., & Lerch, J. P. (2014). Genetic effects on cerebellar structure across mouse models of autism using a magnetic resonance imaging atlas. *Autism research*, *7*(1), 124-137.

Susuki, K. (2010). Myelin: a specialized membrane for cell communication. *Nature Education*, *3*(9), 59.

Susuki, K., & Rasband, M. N. (2008). Molecular mechanisms of node of Ranvier formation. *Current opinion in cell biology*, *20*(6), 616-623.

Suzuki, S., Jensen, E. L., Bossaerts, P., & O'Doherty, J. P. (2016). Behavioral contagion during learning about another agent's risk-preferences acts on the neural representation of decision-risk. *Proceedings of the National Academy of Sciences*, *113*(14), 3755-3760.

Taveggia, C., Feltri, M. L., & Wrabetz, L. (2010). Signals to promote myelin formation and repair. *Nature Reviews Neurology*, *6*(5), 276-287.

Tomlinson, L., Leiton, C. V., & Colognato, H. (2016). Behavioral experiences as drivers of oligodendrocyte lineage dynamics and myelin plasticity. *Neuropharmacology*, *110*, 548-562.

Turati, L., Moscatelli, M., Mastropietro, A., Dowell, N. G., Zucca, I., Erbetta, A., Cordiglieri, C., Brenna, G., Bianchi, B., Mantegazza, R., Cercignani, M., Baggi, F., & Minati, L. (2015). In vivo quantitative magnetization transfer imaging correlates with histology during de- and remyelination in cuprizone-treated mice. *NMR Biomed*, *28*(3), 327-337. https://doi.org/10.1002/nbm.3253

Ullmann, J. F., Watson, C., Janke, A. L., Kurniawan, N. D., & Reutens, D. C. (2013). A segmentation protocol and MRI atlas of the C57BL/6J mouse neocortex. *Neuroimage*, *78*, 196-203.

Uschkureit, T., Spörkel, O., Stracke, J., Büssow, H., & Stoffel, W. (2000). Early onset of axonal degeneration in double (plp−/− mag−/−) and hypomyelinosis in triple (plp−/− mbp−/− mag−/−) mutant mice. *Journal of Neuroscience*, *20*(14), 5225-5233.

Weiss, I. C., Pryce, C. R., Jongen-Rêlo, A. L., Nanz-Bahr, N. I., & Feldon, J. (2004). Effect of social isolation on stress-related behavioural and neuroendocrine state in the rat. *Behavioural brain research*, *152*(2), 279-295.

Wolff, S. D., & Balaban, R. S. (1989). Magnetization transfer contrast (MTC) and tissue water proton relaxation in vivo. *Magnetic resonance in medicine*, *10*(1), 135-144.

Wolff, S. D., & Balaban, R. S. (1989). Magnetization transfer contrast (MTC) and tissue water proton relaxationin vivo. *Magnetic resonance in medicine*, *10*(1), 135-144. https://doi.org/10.1002/mrm.1910100113

Yizhar, O., Fenno, L. E., Prigge, M., Schneider, F., Davidson, T. J., O'shea, D. J., Sohal, V. S., Goshen, I., Finkelstein, J., & Paz, J. T. (2011). Neocortical excitation/inhibition balance in information processing and social dysfunction. *Nature*, *477*(7363), 171-178.

Zeighami, Y., Fereshtehnejad, S.-M., Dadar, M., Collins, D. L., Postuma, R. B., Mišić, B., & Dagher, A. (2019). A clinical-anatomical signature of Parkinson's disease identified with partial least squares and magnetic resonance imaging. *Neuroimage*, *190*, 69-78.